Default Mode Network Mechanisms of Transcranial Magnetic Stimulation in Depression

Supplement 1

Supplementary Methods

Subjects

Seventeen outpatients meeting DSM-IV TR criteria for a non-psychotic major depressive episode (mean age 42.3, SD = 17.3; 18% male) and 35 healthy control subjects (mean age 36.0, SD = 16.0; 34% male) participated in this study after providing informed consent. These groups did not differ significantly in terms of age (t = 1.24, p = 0.21) or sex (t = 1.21, p = 0.20). (To further control for age- and sex-related variability, we included these variables as covariates in our resting state fMRI analyses, as described below.) Patients were referred by the outpatient clinic in the Department of Psychiatry at Weill Cornell Medical College. Patients were also self-referred by directly contacting our transcranial magnetic stimulation (TMS) program. Healthy control subjects were recruited from the local community via flyers, outreach at local events, or direct contact. The recruitment procedure and all other aspects of our experimental protocol were approved by the Institutional Review Board of Weill Cornell Medical College, and all experiments were conducted in accordance with institutional guidelines and regulations.

All subjects participated in an initial screening interview to determine eligibility for enrollment in the study. Potential subjects were excluded from the study if they presented with a history of claustrophobia, seizure disorder or other neurological disorder, head injury resulting in loss of consciousness, metal implants, pacemakers,

intrauterine contraceptive devices, or braces, or if they were currently pregnant or lactating. Subjects were eligible for inclusion as healthy controls if they also presented without any history of psychiatric illness. Patients were eligible for inclusion in the study if they currently met DSM-IV-TR criteria for a major depressive episode with a diagnosis of major depressive disorder (MDD) or bipolar II disorder. Diagnoses were determined by a Board-Certified psychiatrist (MJD) in an unstructured clinical interview and through consultation with family members and the current treating psychiatrist. Patients also met inclusion criteria for treatment-resistance, including a failure to respond to at least two previous antidepressant trials at adequate doses for 8 weeks during the current episode (or two mood stabilizer trials, in the case of a single patient with bipolar II disorder, current episode depressed). In addition to the exclusion criteria for all subjects documented above, patients were excluded if they had bipolar I disorder or a psychotic disorder, were actively suicidal with plan or intent, had been in their current episode for longer than 3 years, had a history of clinically significant personality disorder as established in the diagnostic interview, or had substance abuse disorder or substance dependence within the past 3 years.

Diagnostic and medication history for the patient group are described in Table S1. All patients had a history of at least two major depressive episodes, including the current episode. The lifetime number of major depressive episodes averaged 5.3 (SD = 2.6). Three subjects had a history of hypomania and thus had a diagnosis of bipolar II disorder. All other subjects met criteria for major depressive disorder. There were no other Axis I co-morbidities. Participants were allowed to continue prior medications as long as doses remained unchanged for four weeks prior to the beginning of the study as

well as during the course of TMS. Of the 17 patients, 14 were taking antidepressant medications, and some were also taking mood stabilizers, antipsychotics, and other medications (see Table S1 for details). To control for variability associated with individual differences in medication history, we included subjects' history of antipsychotic, mood stabilizer, and antidepressant trials as covariates in our fMRI analysis, as described below.

TMS Protocol

All 17 patients completed 25 sessions of TMS over the left dorsolateral prefrontal cortex (DLPFC) over a 5-week period using the NeuroStar TMS Therapy System (Neuronetics, Inc.). We assessed treatment response using the 24-item Hamilton Rating Scale for Depression (HAM-D) at baseline and 1–3 days after completing the 5-week course of treatment. Individual sessions consisted of 37.5 min (3000 pulses; 30-second duty cycle, 4 seconds on, 26 seconds off) of 10-Hz excitatory TMS daily for 25 days (Monday-Friday for a 5 week period), as described in previous randomized controlled trials (1). The TMS coil (Neuronetics Neurostar System, standard Figure 8 coil, www.neuronetics.com) was centered over the scalp using the Beam F3 method based on surface distances between the nasion, inion, tragus and vertex as landmarks (2). Resting motor threshold (MT) was defined as the stimulus strength over the thumb area of motor cortex that produced visually detectable thumb movement on 50% of trials. MT was measured prior to the first treatment and on every fifth treatment thereafter, based on our observation that MT tends to decrease slightly over a 5-week course of treatment. We aimed to apply repetitive stimulation at 120% of the resting

motor threshold (3), and all subjects except two tolerated intensities of 80-120% (mean 91.3%, SD = 9.9%). Resting motor thresholds and stimulation intensity for each subject are described in Table S2. To control for variability associated with individual differences in stimulation intensity, we included this variable as a covariate in our fMRI analysis, as described below.

Resting State (rs)-fMRI Data Acquisition

MRI data were obtained from patients in two sessions that occurred before (mean 2.8 days, SD 2.1 days) and shortly after (mean 1.4 days, SD 1.3 days) completing the 5-week course of TMS. MRI data were obtained from healthy control subjects in a single session. Each scanning session was conducted on a 3-T GE scanner (General Electric, Milwaukee, WI) at Weill Cornell and included an rs-fMRI sequence (240 mm field of view, 64 x 64 voxel acquisition matrix x 28 slices, TR = 2.0 s, echo time = 40 ms, 180 volumes) and a high-resolution T1-weighted (MP-RAGE) anatomical scan (256 mm field of view, 256 x 256 voxel acquisition matrix). Anatomical scans were acquired in each session for between-session co-registration and for transformation of subjects' imaging data into a common space for group statistics.

Data Preprocessing

Preprocessing of rs-fMRI data was conducted with the AFNI (http://afni.nimh.nih.gov/afni/) and FSL (http://www.fmrib.ox.ac.uk/fsl/) software packages and included motion correction (AFNI), spatial smoothing (6-mm full-width half-maximum Gaussian kernel; FSL), temporal band-pass filtering (0.005-0.1 Hz;

AFNI), linear and quadratic detrending (AFNI), and removal of nuisance signals by regression on six motion parameters (roll, pitch, yaw, and translation in three dimensions) and signal time courses for white matter and cerebrospinal fluid (CSF) regions-of-interest (ROIs) determined on an individual basis using an automated segmentation algorithm (FSL). We did not regress on the global signal time course (4). The white matter and CSF regions-of-interest encompassed only a small proportion of all brain voxels that was comparable between groups (CSF: 0.4% in controls, 0.3% in MDD; white matter: 3.8% in controls, 2.9% in MDD). To rule out the possibility that individual differences in the CSF and white matter masks could have confounded between-group differences in functional connectivity, we tested for voxelwise differences in the coefficient of partial determination (R^2) for these regressors, and found that there were no significant differences between patients and controls in the variance removed by regressing on the white matter and CSF signal time courses. To further control for motion effects, we quantified head movement in each subject's resting state fMRI scan in terms of the root-mean-square of these six parameters (averaged over the time series), and included this variable as a covariate in our analyses, as described below.

Subjects' pre-processed functional data were co-registered to their high-resolution T1 anatomical data and then transformed into standard Montreal Neurological Institute (MNI) space using FSL's linear image registration tool (FLIRT) and trilinear interpolation. The results of the co-registration and transformation steps were visually inspected. Furthermore, each dataset was assessed for loss-of-signal artifacts—especially important in this study because the subgenual cingulate (sgACC) may be

particularly susceptible due to its adjacency to air sinuses—by calculating maps of the temporal signal-to-noise ratio (SNR: the voxelwise mean of the MR signal over time divided by the standard deviation of the time series). Datasets were excluded from further analysis if the SNR averaged over all voxels in any of the regions-of-interest defined below was less than 40 (5). In all subjects, the SNR exceeded this threshold in the subgenual cingulate ROI (Figure S1A). However, in one patient, there was significant loss of signal over the lateral cortical convexities bilaterally (Figure S1A-C), and this subject was excluded from subsequent analyses.

Data Analysis

To test for functional connectivity differences in depression and for effects of TMS, we generated functional connectivity maps between seeds in the left DLPFC and subgenual cingulate cortex and targets in the central executive network (CEN) and default mode network (DMN). ROIs comprising the DMN (Figure S2) and CEN (Figure S3) were defined *a priori* based on the results of an independent components analysis of 90 healthy human subjects in a previously published report (6). The sgACC seed was an ROI within Brodmann's area (BA) 25 (9-mm seed centered on MNI coordinates: 2, 18, –8). We selected this seed because functional connectivity between sgACC and dorsolateral prefrontal stimulation sites has been implicated in the response to TMS (7). Neuronal activity in this structure is frequently increased in depression (8-13) and is sensitive to treatment in multiple different modalities (12-18). Furthermore, although the sgACC does not lie within the DMN, sgACC and DMN activity are highly correlated, especially in depression (9, 10). The precise coordinates were defined *a priori* using an

average of the coordinates that were implicated in depression in previously published papers (Table S3) (7, 9, 10, 12-19). The left DLPFC seed was an ROI within BA46 (9-mm seed centered on MNI coordinates: –44, 40, 29). Activity in the left DLPFC is consistently decreased in depression (20-22). Again, we selected the coordinates for this seed based on a previous study (7), in which BA46 and its connectivity with sgACC were implicated in the response to TMS. We did not employ an MRI-based neuro-navigation system, which would allow us to determine whether the DLPFC seed and stimulation site were precisely co-localized; however, these coordinates were predicted to lie within the stimulation field, which was ~3 cm in diameter and located ~5 cm anterior to the hand area of primary motor cortex (estimated to occur at MNI coordinates +/–38, –22, 58 (23)). This seed lies adjacent to the CEN as defined in a prior report but not within it (6); however, activity in BA46 is highly correlated with activity throughout the CEN and plays a critical role in cognitive control processes (6, 10).

Thus, we used seeds in the left DLPFC and subgenual cingulate cortex that are closely linked to activity in the CEN and DMN, respectively, and tested for effects on connectivity with targets in large CEN and DMN masks, resulting in two within-network connectivity maps (DLPFC:CEN, sgACC:DMN) and two between-network connectivity maps (DLFPC:DMN, and sgACC:CEN). These connectivity maps were the focus of our group-level analyses, which were conducted in AFNI. To test for differences in functional connectivity between patients and healthy controls in each of these four maps, we used analysis of covariance (ANCOVA) comparing patients vs. controls, with age, sex, and head movement (see above) as covariates. To test for effects of TMS on functional connectivity, we used repeated measures ANCOVA, contrasting each

subject's pre-treatment connectivity map with his or her post-treatment map, covarying for factors that may contribute to treatment response, including age, sex, baseline HAM-D score, TMS intensity (% of resting motor threshold), history of antipsychotic or mood stabilizer use, and lifetime number of antidepressant trials as a proxy for treatment resistance. We also tested for normalization of differences that were observed prior to treatment by comparing patients' post-treatment connectivity maps with healthy controls (ANCOVA, covariates as above: age, sex, head movement). Finally, to test whether baseline connectivity maps were related to subsequent treatment response, we divided patients into two groups based on a median split of the percent change in HAM-D ($[\text{HAM-D}_{\text{post-treatment}} - \text{HAM-D}_{\text{pre-treatment}}] / \text{HAM-D}_{\text{pre-treatment}}$), and tested for differences in their baseline functional connectivity maps (ANCOVA, covariates: age, sex, baseline HAM-D score, and lifetime number of antidepressant trials). In all analyses, significant effects were identified using a cluster threshold to correct for multiple comparisons (24). The cluster threshold criteria ($K > 16$ voxels, $p < 0.01$ for network-of-interest analyses; $K > 25$, $p < 0.005$ for whole brain analyses) were selected based on Monte Carlo simulation of a random field of noise to ensure an overall alpha probability of a type I error of < 0.05.

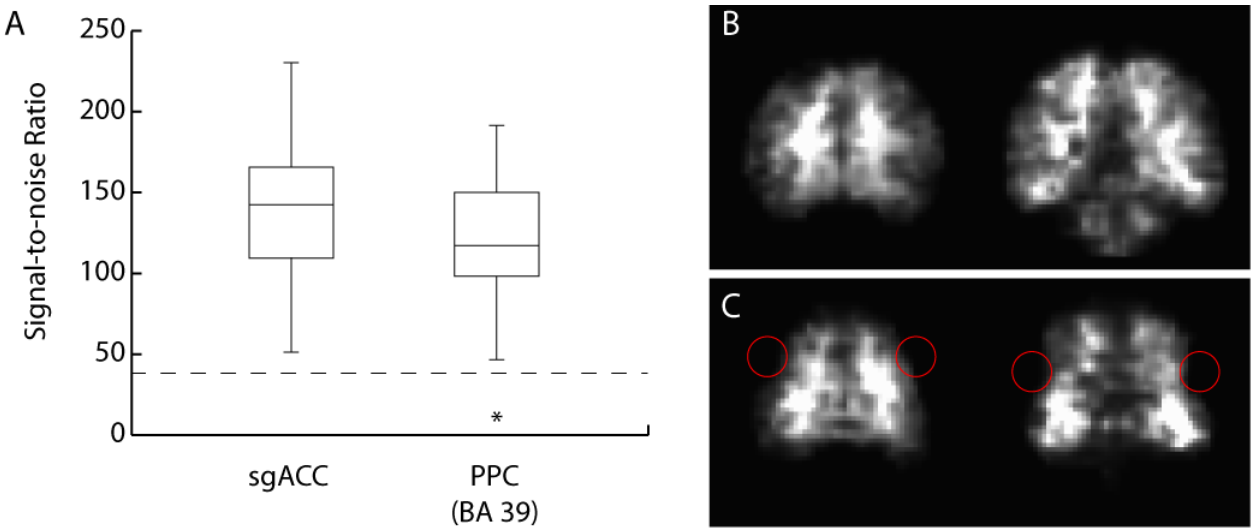

Figure S1. Data quality assessment. Each dataset was assessed for loss-of-signal artifact—especially important in this study because the subgenual cingulate (sgACC) may be susceptible due to its adjacency to air sinuses—by calculating maps of the temporal signal-to-noise ratio (SNR: the voxelwise mean of the MR signal over time divided by the standard deviation of the time series). Datasets were excluded from further analysis if the SNR averaged over all voxels in any of the regions-of-interest (ROI) defined below was less than 40. **(A)** In all subjects, the SNR exceeded this threshold in the subgenual cingulate ROI. However, in one patient (outlier denoted by an asterisk), there was significant loss of signal over the lateral cortical convexities bilaterally, as depicted in this example ROI located in the posterior parietal cortex (PPC). **(B)** SNR maps (coronal images) for a typical subject. **(C)** SNR maps from the subject who was excluded due to loss of signal over the lateral cortical convexities bilaterally for comparison with (B). Red circles indicate areas with significant loss of signal. BA, Brodmann area.

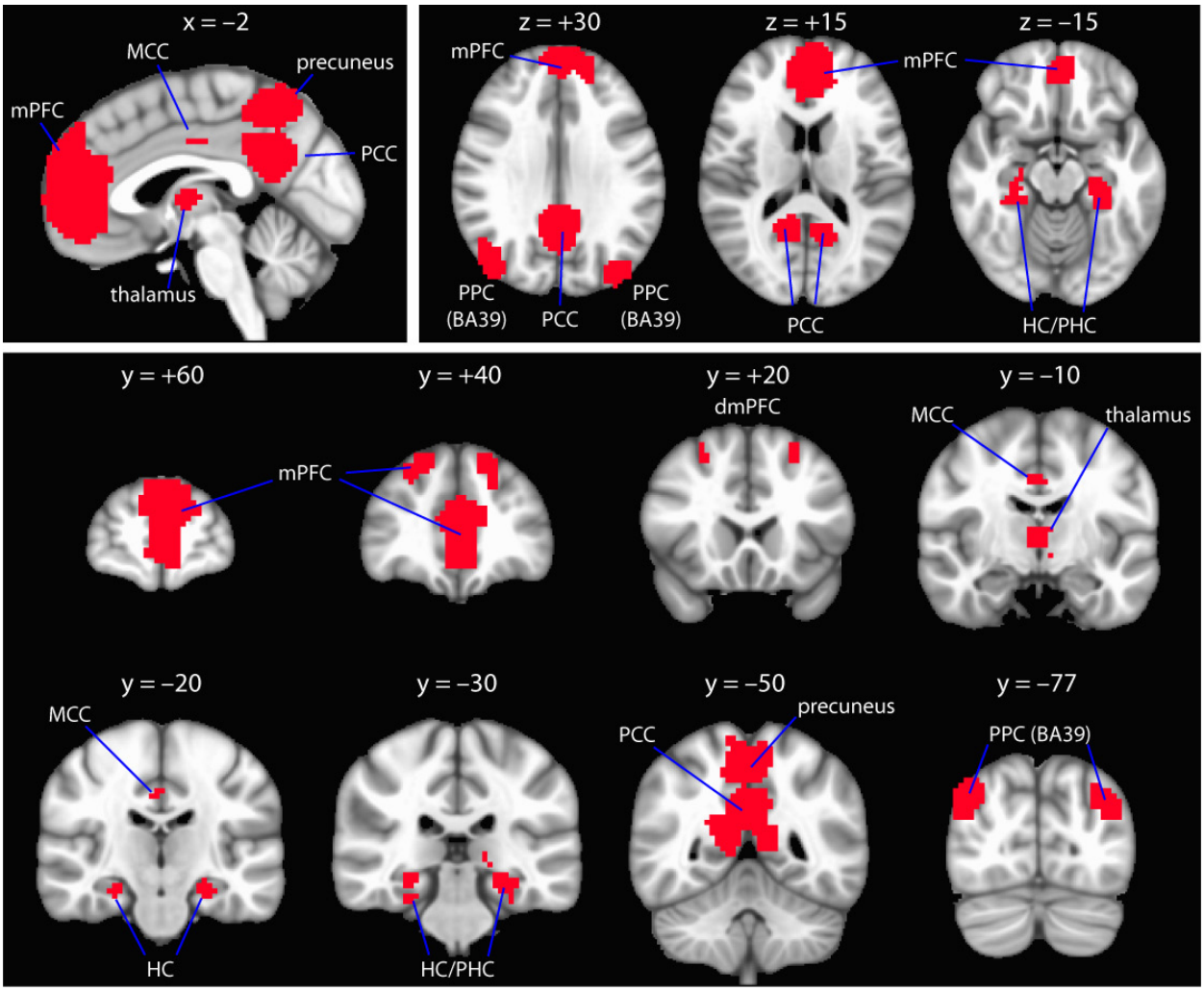

Figure S2. The default mode network (DMN). Connectivity target regions of interest comprising the DMN were defined *a priori* based on the results of an independent components analysis of 90 healthy human subjects in a previously published report (20). Components of this network are depicted below. BA, Brodmann area; dmPFC, dorsomedial prefrontal cortex; HC, hippocampus; MCC, middle cingulate cortex; mPFC, medial prefrontal cortex; PCC, posterior cingulate cortex; PHC, parahippocampal cortex; PPC, posterior parietal cortex.

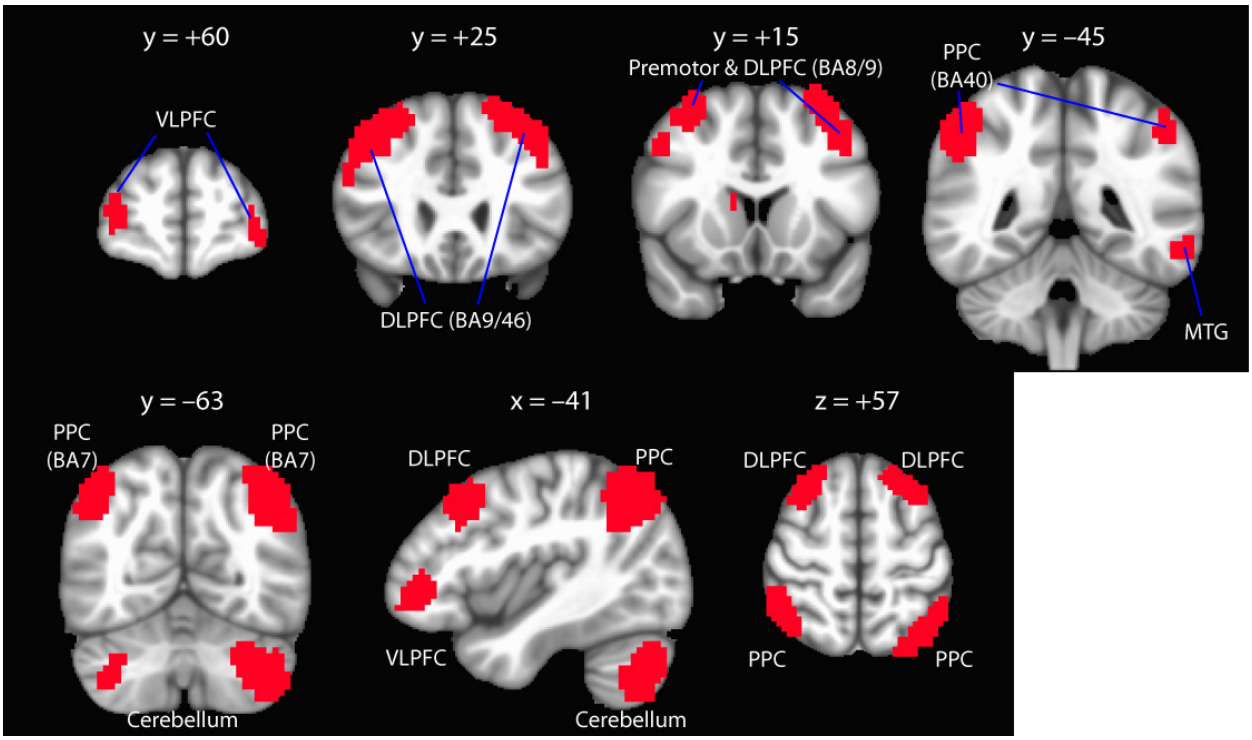

Figure S3. The central executive network (CEN). Connectivity target regions of interest comprising the CEN were defined *a priori* based on the same analysis described above (20). Components of this network are depicted below. BA, Brodmann area; DLPFC, dorsolateral prefrontal cortex; MTG, middle temporal gyrus; PPC, posterior parietal cortex; VLPFC, ventrolateral prefrontal cortex. Note that the posterior parietal areas of the CEN (BA40, BA7) depicted here are neuroanatomically distinct from the posterior parietal areas of the DMN (BA39) depicted in Figure S1.

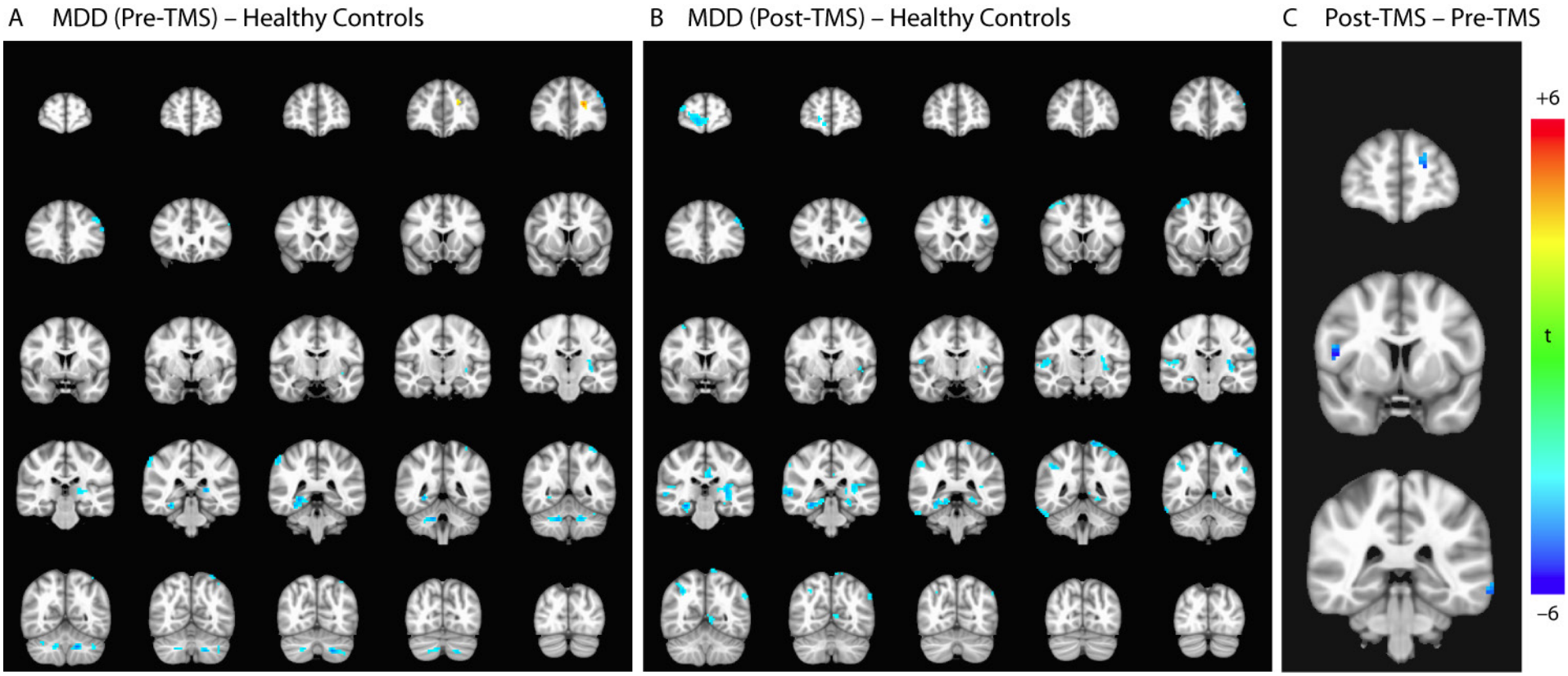

Figure S4. Unmasked whole-brain analyses of dorsolateral prefrontal cortex (DLPFC) connectivity before and after transcranial magnetic stimulation (TMS). (A) Prior to treatment, depressed patients exhibited widespread reductions in DLPFC functional connectivity, especially within areas of the central executive network and default mode network (DMN) that converge with the region of interest (ROI) analyses depicted in Figures 1 and 3. **(B)** These effects tended to persist after treatment. **(C)** In accord with the ROI analysis depicted in Figure 3E, TMS significantly reduced functional connectivity between the DLPFC and dorsomedial prefrontal areas of the DMN. MDD, major depressive disorder.

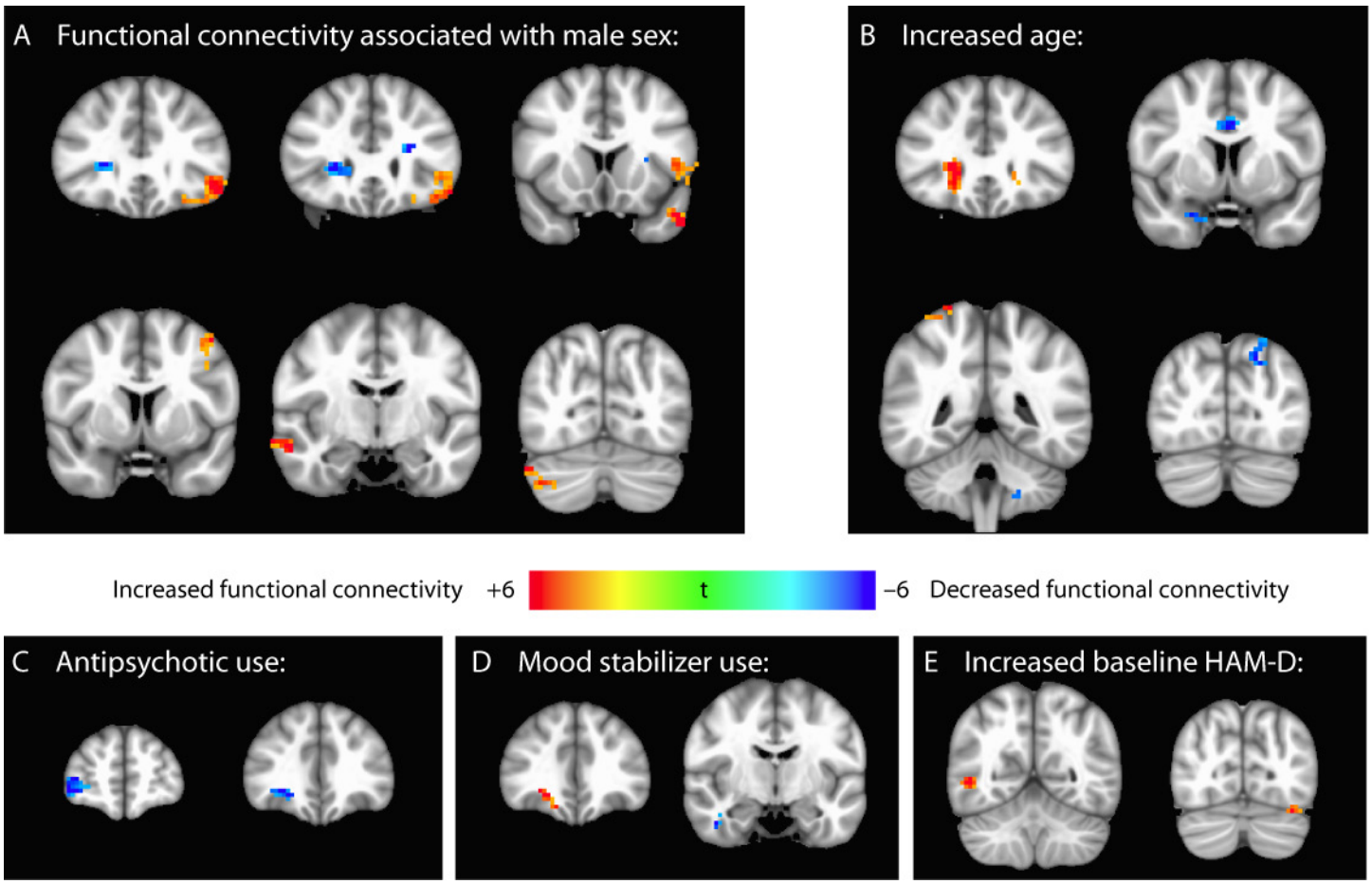

Figure S5. Covariate effects on dorsolateral prefrontal cortex (DLPFC) connectivity prior to treatment. Pre-treatment DLPFC connectivity was modulated by sex **(A)**, age **(B)**, antipsychotic use **(C)**, mood stabilizer use **(D)**, and depression severity (**E**: baseline Hamilton Rating Scale for Depression (HAM-D) score) in the areas depicted above. Treatment refractoriness (number of failed antidepressant trials) was not significantly correlated with subgenual cingulate connectivity.

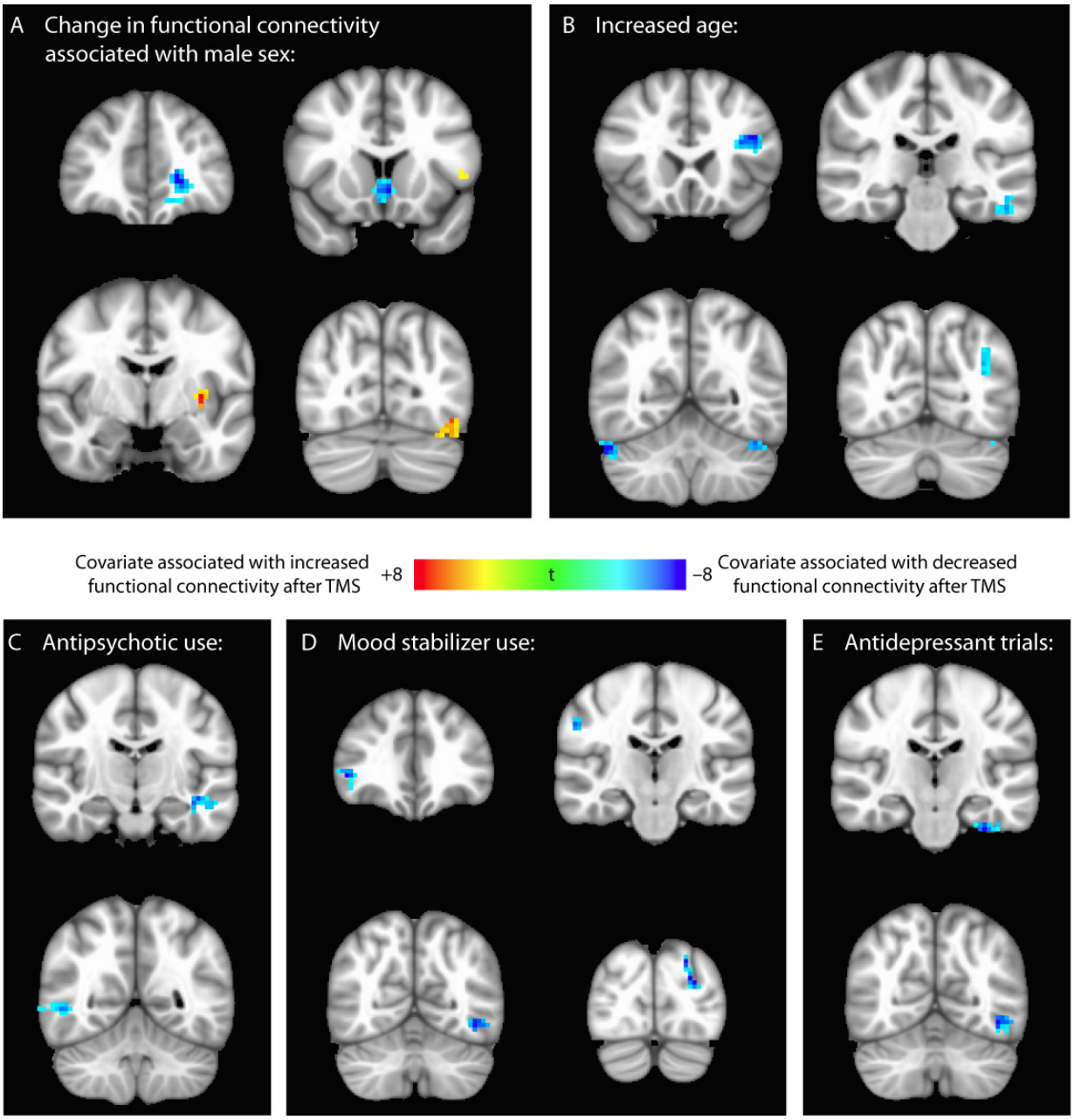

Figure S6. Covariate effects on transcranial magnetic stimulation (TMS)-related changes in dorsolateral prefrontal cortex (DLPFC) connectivity. TMS effects on DLPFC connectivity (pre-treatment versus post-treatment changes) were modulated by sex **(A)**, age **(B)**, antipsychotic use **(C)**, mood stabilizer use **(D)**, and treatment refractoriness (**E**: # of failed antidepressant trials). The effects of TMS on DLPFC connectivity depicted in Figure 3E-F occurred independently of these covariates in a repeated measures analysis of covariance. Depression severity (baseline Hamilton Rating Scale for Depression score) was not significantly correlated with subgenual cingulate connectivity.

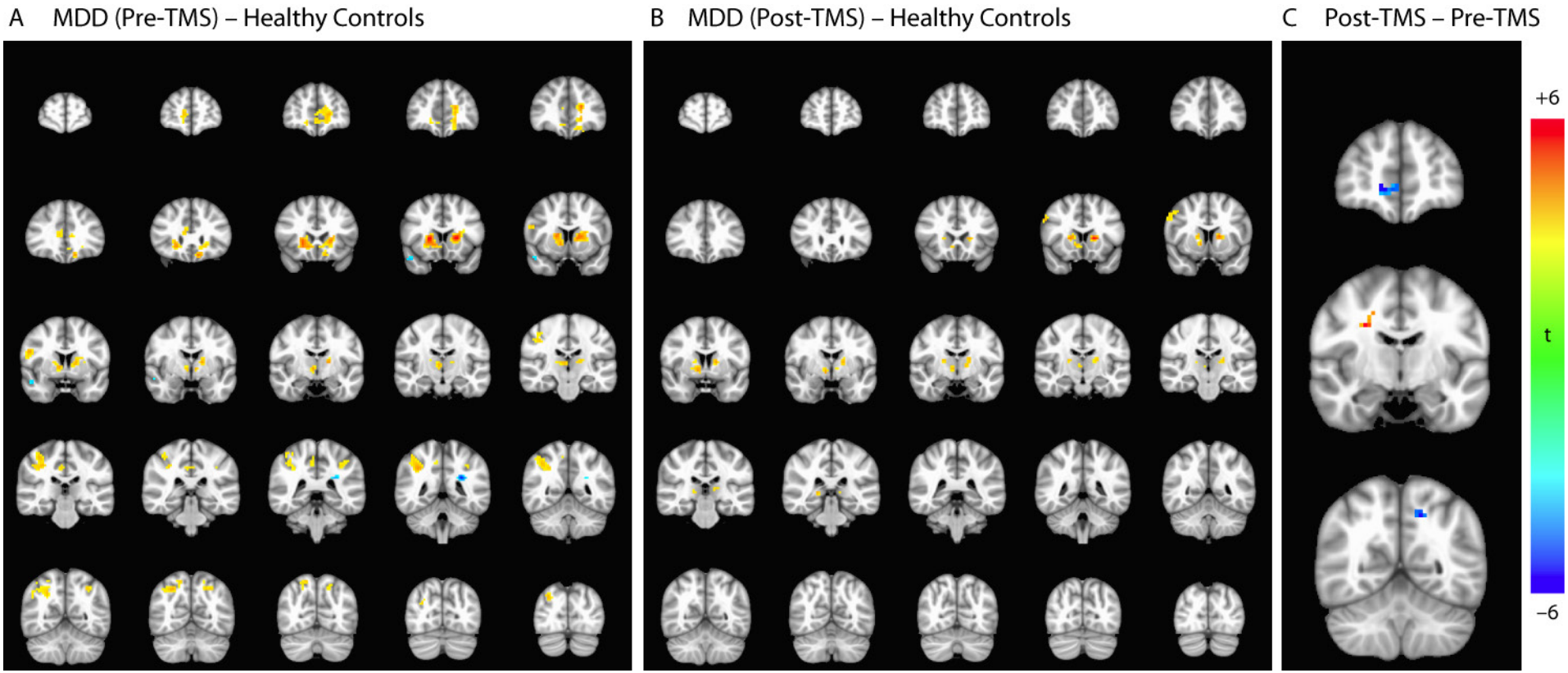

Figure S7. Unmasked whole-brain analyses of subgenual cingulate (sgACC) connectivity before and after transcranial magnetic stimulation (TMS). **(A)** Prior to treatment, sgACC connectivity was abnormally elevated in depressed patients, especially within areas of the default mode network (DMN) and central executive network that converge with the region of interest (ROI) analyses depicted in Figures 2 and 3. **(B)** These abnormalities tended to resolve after treatment. A notable exception was persistently elevated sgACC connectivity with subcortical areas including the thalamus, bilateral caudate, and ventral striatum. **(C)** In accord with the ROI analysis depicted in Figure 2C, TMS attenuated depression-related hyperconnectivity between the sgACC and multiple areas of the DMN. MDD, major depressive disorder.

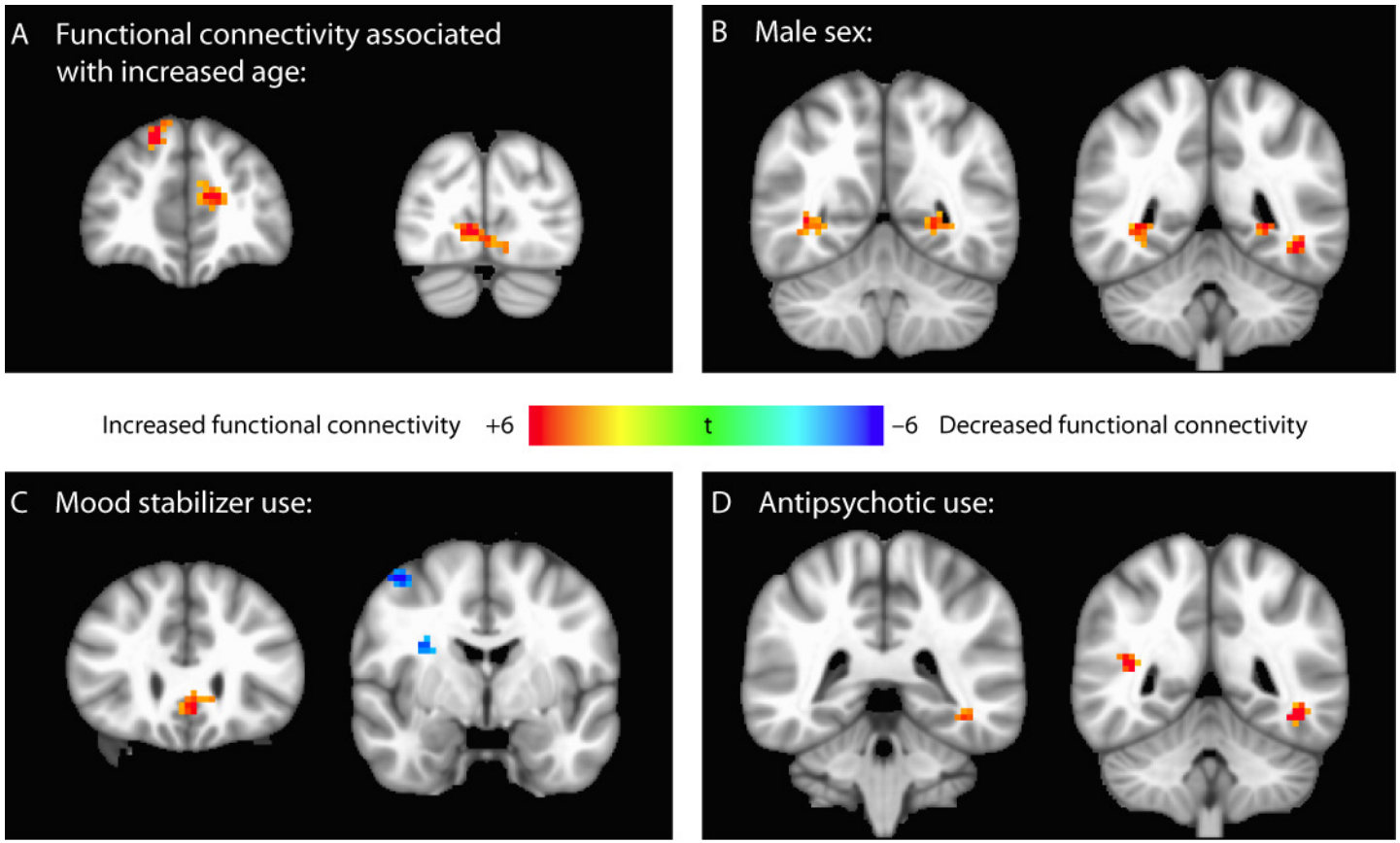

Figure S8. Covariate effects on subgenual cingulate (sgACC) connectivity prior to treatment. Pre-treatment sgACC connectivity was modulated by age **(A)**, sex **(B)**, mood stabilizer use **(C)**, and antipsychotic use **(D)** in the areas depicted above. Depression severity (baseline Hamilton Rating Scale for Depression score) and treatment refractoriness (number of failed antidepressant trials) were not significantly correlated with sgACC connectivity.

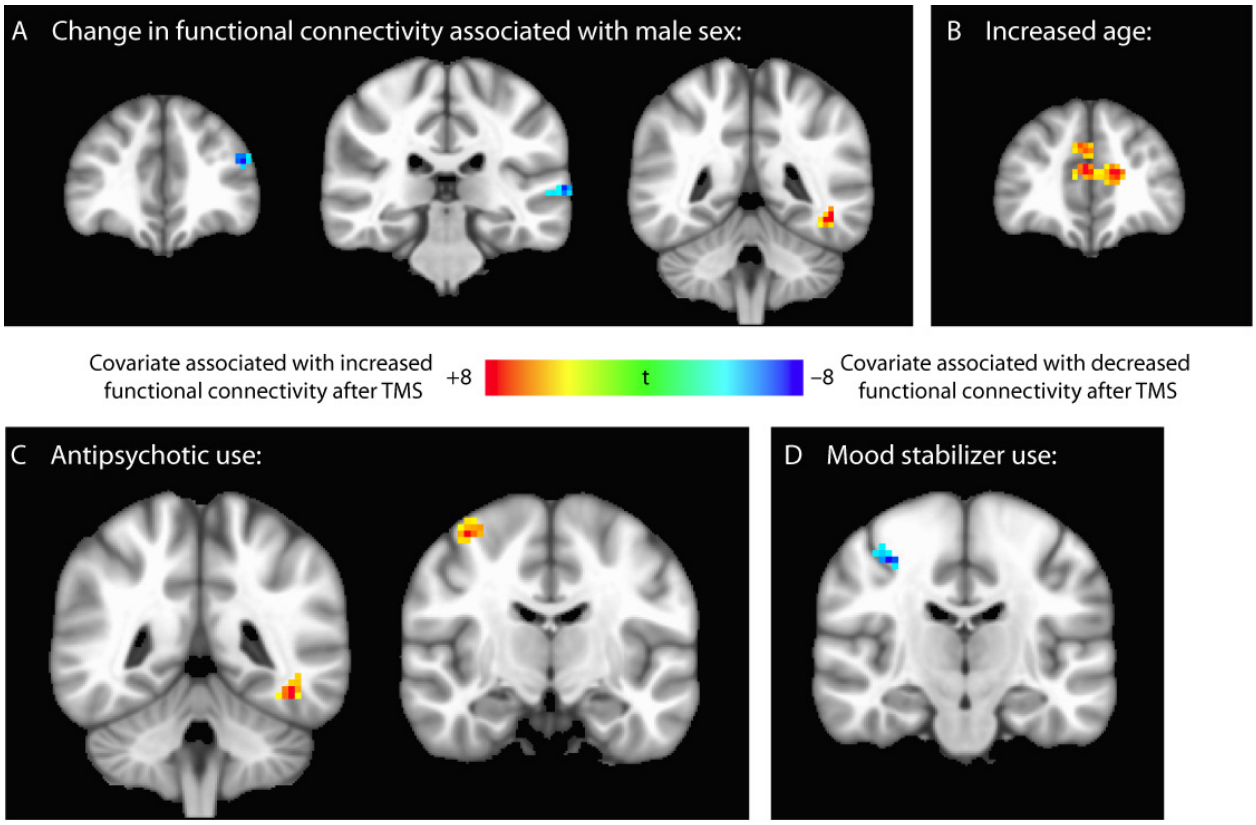

Figure S9. Covariate effects on transcranial magnetic stimulation (TMS)-related changes in subgenual cingulate (sgACC) connectivity. TMS effects on sgACC connectivity (pre-treatment versus post-treatment changes) were modulated by sex **(A)**, age **(B)**, antipsychotic use **(C)**, and mood stabilizer use **(D)** in the areas depicted above. The effects of TMS on sgACC connectivity depicted in Figure 2C-D occurred independently of these covariates in a repeated measures analysis of covariance. Depression severity (baseline Hamilton Rating Scale for Depression score) and treatment refractoriness (number of failed antidepressant trials) were not significantly correlated with TMS-related changes in sgACC connectivity.

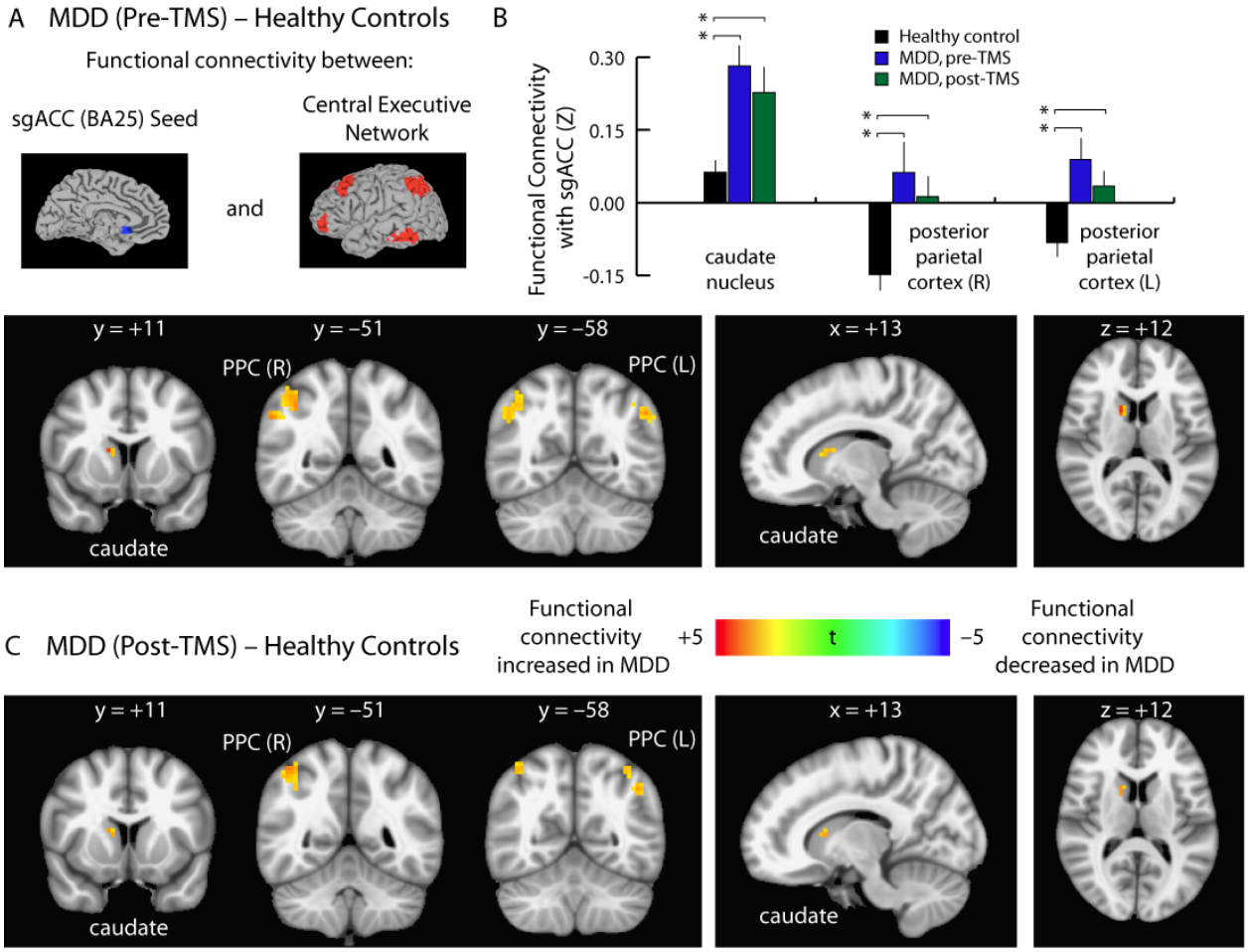

Figure S10. Transcranial magnetic stimulation (TMS) modulates interactions between the default mode network and central executive network (CEN). (A) Compared to healthy control subjects, functional connectivity between the subgenual cingulate (sgACC) and the CEN was abnormally elevated in depressed patients. Affected areas included the right caudate nucleus and bilateral posterior parietal cortex (PPC, BA40). Images depict *t* statistics for the contrast of patients prior to treatment versus healthy controls. This data was presented in Figure 3 and is illustrated here to facilitate a comparison with panel C. **(B-C)** Hyperconnectivity with the right caudate and bilateral posterior parietal cortex persisted after treatment. Error bars = SEM. *$p < 0.05$, corrected for multiple comparisons. BA, Brodmann area; MDD, major depressive disorder; L, left; R, right.

Table S1. Age, sex, axis I DSM-IV diagnosis, current medications (total daily dose in milligrams), number of lifetime and current episode trials of adequate dose and duration for antidepressant, mood stabilizer and antipsychotic medication classes.

					Medication Trials: Lifetime (Current Episode)		
Subject	**Age**	**Sex**	**Axis I**	**Current Medications**	**Antidepressant**	**Mood Stabilizer**	**Antipsychotic**
1	52	F	Bipolar II, Depressed	Clonazepam 1mg	5 (5)	0	1 (1)
2	68	M	MDD	Duloxetine 60mg Bupropion 300mg Lamotrigine 200mg	3 (2)	1 (1)	1 (0)
3	24	F	MDD	Venlafaxine 450mg Aripiprazole 15mg Lorazepam 0.5mg PRN	5 (5)	1 (1)	2 (2)
4	41	F	MDD	Dextroamphetamine 15mg Zolpidem 10mg	7 (6)	0	5 (5)
5	67	F	MDD	Methylphenidate 20mg	2 (2)	1 (1)	1 (1)
6	41	F	Bipolar II, Depressed	Fluvoxamine 400mg Topiramate 100mg Quetiapine 200mg Ziprasidone 160mg Perphenazine 32mg Lorazepam 2mg	4 (4)	1 (1)	4 (4)
7	53	F	MDD	Duloxetine 60mg Bupropion 150mg	5 (2)	0	0
8	26	M	MDD	Fluoxetine 60mg Bupropion 450mg Topiramate 100mg	2 (2)	1 (1)	0

					Medication Trials: Lifetime (Current Episode)		
Subject	**Age**	**Sex**	**Axis I**	**Current Medications**	**Antidepressant**	**Mood Stabilizer**	**Antipsychotic**
9	20	F	Bipolar II, Depressed	Lithium 900mg Pramipexole 6mg Pregabalin 450mg Lamotrigine 200mg Aripiprazole 5mg	0	4 (4)	2 (2)
10	68	F	MDD	Venlafaxine 300mg Citalopram 40mg Clomipramine 50mg Gabapentin 2400mg Clonazepam 0.5mg	3 (3)	1 (1)	0
11	40	M	MDD	Venlafaxine 75mg Bupropion 100mg Lorazepam 1mg	3 (3)	0	0
12	27	F	MDD	None	5 (2)	0	0
13	56	F	MDD	None	2 (2)	1 (1)	1 (1)
14	22	F	MDD	Sertraline 200mg	6 (2)	1 (0)	1 (0)
15	24	F	MDD	Sertraline 200mg Bupropion 150mg	5 (5)	0	2 (2)
16	33	F	MDD	None	7 (4)	1 (0)	2 (1)
17	60	F	MDD	Tranylcypromine 40mg Dextroamphetamine 5mg Clonazepam 0.5mg	7 (6)	0	1 (1)

F, female; M, male; MDD, major depressive disorder.

Table S2. Average stimulation intensity (percent resting motor threshold; %MT) over the left dorsolateral prefrontal cortex during the 5-week course of TMS. Baseline and % change in Hamilton Rating Scale for Depression (HAMD-24) score during the 5-week course of TMS.

		HAMD-24	
Subjec	**%MT**	**Baseline**	**% Change**
1	95	33	-33%
2	85	16	13%
3	101	24	-63%
4	50	31	-19%
5	100	22	-59%
6	81	36	-28%
7	85	27	-44%
8	95	24	-25%
9	109	26	0%
10	86	18	0%
11	107	28	-29%
12	83	25	-84%
13	50	25	-88%
14	98	37	-54%
15	85	17	0%
16	80	16	-13%
17	80	33	-33%

Table S3. The coordinates for the subgenual cingulate seed were defined *a priori* based on an average of the coordinates that were implicated in depression in the following previously published studies. Reference numbers refer to the reference list in the main text. X, Y, and Z refer to Montreal Neurological Institute coordinates.

Study	**Ref #**	**X**	**Y**	**Z**
Fox *et al.* (2012)	10	6	16	-10
Sheline *et al.* (2010)	24	10	35	-2
Sheline *et al.* (2010)	24	-30	35	-2
Greicius *et al.* (2007)	26	-10	5	-10
Mayberg *et al.* (2005)	33	-2	9	-11
Mayberg *et al.* (2005)	33	10	21	-4
Mayberg *et al.* (2000)	34	4	2	-5
Drevets *et al.* (2002)	45	3	32	-10
Kito *et al.* (2008)	46	17	17	-16
Nahas *et al.* (2007)	47	0	9	-19
Wu *et al.* (1999)	48	7	18	-4
Kito *et al*. (2011)	49	8	22	-9
Mayberg *et al.* (1999)	50	0	22	-2
Mayberg *et al.* (1999)	50	-2	6	-6
Average		1.5	17.8	-7.9

Table S4. Depression-related differences in functional connectivity between dorsolateral prefrontal cortex and central executive network nodes. Data accompanies Figure 1. X, Y, and Z refer to coordinates of peak *t* statistic for each cluster in Montreal Neurological Institute space.

Cluster	BA	X	Y	Z	*t*
MDD (Pre-TMS) – Healthy Controls					
Left DLPFC	8/9/6	-27	27	51	-3.51
Right DLPFC & premotor	8/9/6	42	33	48	-3.46
Right PPC	40	57	-39	51	-3.79
Left PPC	40	-48	-45	42	-3.00
Left PPC	7	-39	-66	60	-3.40
Left cerebellum	NA	27	-69	-45	-3.60
Right cerebellum	NA	39	-72	-42	-3.18
MDD (Post-TMS) – Healthy Controls					
Left DLPFC	8/9/6	-42	21	33	-4.24
Right DLPFC & premotor	8/9/6	36	12	57	-4.47
Right PPC	40	42	-48	42	-3.81
Left PPC	40	-51	-51	36	-3.34
Left PPC	7	-30	-69	57	-3.49
MDD (Pre-TMS) – MDD (Post-TMS)					
No significant effects					

BA, Brodmann area; DLPFC, dorsolateral prefrontal cortex; MDD, major depressive disorder; PPC, posterior parietal cortex; TMS, transcranial magnetic stimulation.

Table S5. Depression-related differences in functional connectivity between subgenual cingulate cortex and default mode network nodes. Data accompanies Figure 2. X, Y, and Z refer to coordinates of peak t statistic for each cluster in Montreal Neurological Institute space.

Cluster	BA	X	Y	Z	*t*
MDD (Pre-TMS) – Healthy Controls					
Bilateral vmPFC	10	-18	42	15	4.82
Bilateral pgACC	24	6	30	18	3.29
Right thalamus	na	6	-9	0	4.32
Right precuneus	7/31	9	-42	48	3.40
MDD (Post-TMS) – Healthy Controls					
Right thalamus	na	6	-9	0	3.82
MDD (Post-TMS) – MDD (Pre-TMS)					
Bilateral pgACC	24/32	3	39	15	-6.94
Bilateral vmPFC	10/32	5	51	-3	-5.07
Left vmPFC	10/32	-9	36	-6	-5.27

BA, Brodmann area; MDD, major depressive disorder; pgACC, pregenual anterior cingulate cortex; TMS, transcranial magnetic stimulation; vmPFC, ventromedial prefrontal cortex.

Table S6. Depression-related differences in functional connectivity between the default mode and central executive networks. Data accompanies Figure 3 and Figure S3. X, Y, and Z refer to coordinates of peak *t* statistic for each cluster in Montreal Neurological Institute space.

Cluster	BA	X	Y	Z	*t*
Functional connectivity between sgACC and central executive network					
MDD (Pre-TMS) – Healthy Controls					
Right caudate	na	15	9	12	4.68
Right PPC	40	39	-51	45	3.75
Left PPC	40	-51	-60	39	3.60
MDD (Post-TMS) – Healthy Controls					
Right caudate	na	15	9	12	3.60
Right PPC	40	45	-51	57	3.79
Left PPC	40	45	57	42	3.41
MDD (Pre-TMS) – MDD (Post-TMS)					
No significant effects					
Functional connectivity between DLPFC and default mode network					
MDD (Pre-TMS) – Healthy Controls					
Right PHC	36	30	-36	-15	-4.53
MDD (Post-TMS) – Healthy Controls					
Right vmPFC	10	9	60	-6	-3.48
Right HC/PHC	36/27	27	-27	-15	-4.63
Left HC/PHC	36/27	-24	-33	-9	-3.47
Left PCC	30	-9	-57	6	-3.04
MDD (Pre-TMS) – MDD (Post-TMS)					
Left dmPFC	9	-18	54	18	-5.01
Bilateral vmPFC	10	0	63	-6	-4.12

BA, Brodmann area; DLPFC, dorsolateral prefrontal cortex; dmPFC, dorsomedial prefrontal cortex; HC, hippocampus; MDD, major depressive disorder; PHC, parahippocampal cortex; PPC, posterior parietal cortex; sgACC, subgenual anterior cingulate cortex; TMS, transcranial magnetic stimulation; vmPFC, ventromedial prefrontal cortex.

Table S7. Baseline subgenual cingulate connectivity predicts treatment response. Data accompanies Figure 4. X, Y, and Z refer to coordinates of peak *t* statistic for each cluster in Montreal Neurological Institute space.

Cluster	BA	X	Y	Z	t
Functional connectivity between sgACC and default mode network					
Strong TMS response – Weak TMS response					
Bilateral vmPFC	10	-3	57	3	8.66
Bilateral mOFC	11/10	-4	47	-13	7.12
Bilateral pgACC/dmPFC	32/9	-12	51	9	9.80
Functional connectivity between sgACC and central executive network					
Strong TMS response – Weak TMS response					
Left PPC	40	-33	-30	45	7.63
Right PPC	40	45	-45	36	6.90
Right DLPFC	8/9	33	30	45	7.63
Functional connectivity between DLPFC and default mode network					
Strong TMS response – Weak TMS response					
No significant effects					
Functional connectivity between DLPFC and central executive network					
Strong TMS response – Weak TMS response					
No significant effects					

BA, Brodmann area; DLPFC, dorsolateral prefrontal cortex; dmPFC, dorsomedial prefrontal cortex; mOFC, medial orbitofrontal cortex; pgACC, pregenual anterior cingulate cortex; PPC, posterior parietal cortex; sgACC, subgenual anterior cingulate cortex; TMS, transcranial magnetic stimulation; vmPFC, ventromedial prefrontal cortex.

Supplementary References

1. George MS, Lisanby SH, Avery D, McDonald WM, Durkalski V, Pavlicova M, *et al.* (2010): Daily left prefrontal transcranial magnetic stimulation therapy for major depressive disorder a sham-controlled randomized trial. *Archives of General Psychiatry*. 67:507-516.

2. Beam W, Borckardt JJ, Reeves ST, George MS (2009): An efficient and accurate new method for locating the F3 position for prefrontal TMS applications. *Brain Stimul*. 2:50-54.

3. O'Reardon JP, Solvason HB, Janicak PG, Sampson S, Isenberg KE, Nahas Z, *et al.* (2007): Efficacy and safety of transcranial magnetic stimulation in the acute treatment of major depression: A multisite randomized controlled trial. *Biological Psychiatry*. 62:1208-1216.

4. Chang CE, Glover GH (2009): Effects of model-based physiological noise correction on default mode network anti-correlations and correlations. *Neuroimage*. 47:1448-1459.

5. Kruger G, Glover GH (2001): Physiological noise in oxygenation-sensitive magnetic resonance imaging. *Magnetic Resonance in Medicine*. 46:631-637.

6. Shirer WR, Ryali S, Rykhlevskaia E, Menon V, Greicius MD (2012): Decoding subject-driven cognitive states with whole-brain connectivity patterns. *Cerebral Cortex*. 22:158-165.

7. Fox MD, Buckner RL, White MP, Greicius MD, Pascual-Leone A (2012): Efficacy of transcranial magnetic stimulation targets for depression is related to intrinsic functional connectivity with the subgenual cingulate. *Biological Psychiatry*. 72:595-603.

8. Anand A, Li Y, Wang Y, Wu JW, Gao SJ, Bukhari L, *et al*. (2005): Activity and connectivity of brain mood regulating circuit in depression: A functional magnetic resonance study. *Biological Psychiatry*. 57:1079-1088.

9. Greicius MD, Flores BH, Menon V, Glover GH, Solvason HB, Kenna H, *et al.* (2007): Resting-state functional connectivity in major depression: Abnormally increased contributions from subgenual cingulate cortex and thalamus. *Biological Psychiatry*. 62:429-437.

10. Sheline YI, Price JL, Yan Z, Mintun MA (2010): Resting-state functional MRI in depression unmasks increased connectivity between networks via the dorsal nexus. *Proceedings of the National Academy of Sciences of the United States of America*. 107:11020-11025.

11. Broyd SJ, Demanuele C, Debener S, Helps SK, James CJ, Sonuga-Barke EJS (2009): Default-mode brain dysfunction in mental disorders: A systematic review. *Neuroscience and Biobehavioral Reviews*. 33:279-296.

12. Mayberg HS, Lozano AM, Voon V, McNeely HE, Seminowicz D, Hamani C, *et al.* (2005): Deep brain stimulation for treatment-resistant depression. *Neuron*. 45:651-660.

13. Mayberg HS, Brannan SK, Tekell JL, Silva JA, Mahurin RK, McGinnis S, *et al.* (2000): Regional metabolic effects of fluoxetine in major depression: Serial changes and relationship to clinical response. *Biological Psychiatry*. 48:830-843.

14. Drevets WC, Bogers W, Raichle ME (2002): Functional anatomical correlates of antidepressant drug treatment assessed using PET measures of regional glucose metabolism. *European Neuropsychopharmacology*. 12:527-544.

15. Kito S, Fujita K, Koga Y (2008): Regional cerebral blood flow changes after low-frequency transcranial magnetic stimulation of the right dorsolateral prefrontal cortex in treatment-resistant depression. *Neuropsychobiology*. 58:29-36.

16. Nahas Z, Teneback C, Chae J-H, Mu Q, Molnar C, Kozel FA, *et al.* (2007): Serial vagus nerve stimulation functional MRI in treatment-resistant depression. *Neuropsychopharmacology*. 32:1649-1660.

17. Wu J, Buchsbaum MS, Gillin JC, Tang C, Cadwell S, Wiegand M, *et al.* (1999): Prediction of antidepressant effects of sleep deprivation by metabolic rates in the ventral anterior cingulate and medial prefrontal cortex. *American Journal of Psychiatry*. 156:1149-1158.

18. Kito S, Hasegawa T, Koga Y (2011): Neuroanatomical correlates of therapeutic efficacy of low-frequency right prefrontal transcranial magnetic stimulation in treatment-resistant depression. *Psychiatry and Clinical Neurosciences*. 65:175-182.

19. Mayberg HS, Liotti M, Brannan SK, McGinnis S, Mahurin RK, Jerabek PA, *et al.* (1999): Reciprocal limbic-cortical function and negative mood: Converging PET findings in depression and normal sadness. *American Journal of Psychiatry*. 156:675-682.

20. Davidson RJ, Pizzagalli D, Nitschke JB, Putnam K (2002): Depression: Perspectives from affective neuroscience. *Annual Review of Psychology*. 53:545-574.

21. Bench CJ, Friston KJ, Brown RG, Scott LC, Frackowiak RSJ, Dolan RJ (1992): The anatomy of melancholia - focal abnormalities of cerebral blood-flow in major depression. *Psychological Medicine*. 22:607-615.

22. Baxter LR, Schwartz JM, Phelps ME, Mazziotta JC, Guze BH, Selin CE, *et al.* (1989): Reduction of prefrontal cortex glucose-metabolism common to 3 types of depression. *Archives of General Psychiatry*. 46:243-250.

23. Hayashi MJ, Saito DN, Aramaki Y, Asai T, Fujibayashi Y, Sadato N (2008): Hemispheric asymmetry of frequency-dependent suppression in the ipsilateral

primary motor cortex during finger movement: a functional magnetic resonance imaging study. *Cerebral Cortex*. 18:2932-2940.

24. Forman SD, Cohen JD, Fitzgerald M, Eddy WF, Mintun MA, Noll DC (1995): Improved assessment of significant activation in functional magnetic-resonance-imaging (fMRI) - use of a cluster-size threshold. *Magnetic Resonance in Medicine*. 33:636-647.